10

Luminescent properties investigation of ZBLAN: Er^{3+}/Ho^{3+} fluoride glass under laser excitation at a wavelength of 1.94 μ m

© V.A. Egolin, A.P. Savikin, S.V. Kurashkin, A.V. Marugin

Lobachevsky State University, Nizhny Novgorod, Russia e-mail: vitaly.egolin@mail.ru Received July 08, 2024 Revised May 07, 2025 Accepted June 02, 2025

A series of fluoride glass samples of the composition ZBLAN:1%Er³+, ZBLAN:1%Ho³+, ZBLAN:1%Ho³+, ZBLAN:1%Ho³+, (X = 0.25, 0.5, 1 mol.%) is synthesized. Based on the transmission spectra of the compounds ZBLAN:1%Ho³+ and ZBLAN:1%Er³+, the Judd-Ofelt intensity parameters for Ho³+ and Er³+ ions in synthesized samples are determined. Up-conversion luminescence of ZBLAN:Er³+/Ho³+ glass under excitation Tm³+:YAP- laser radiation with a wavelength of 1.94 μ m is investigated. The up-conversion luminescence spectra of the visible range exhibit bands in the regions of 545 and 655 nm. The highest intensity was observed for the red lines at a wavelength of 655 nm, which correspond to the transitions ${}^4F_{9/2} \rightarrow {}^4I_{15/2}$ of Er³+ ions and ${}^5F_5 \rightarrow {}^5I_8$ of Ho³+ ions. The threshold power density of radiation visualization of Tm³+:YAP-laser decreased with increasing concentration of Ho³+ ions and was 30 W/cm² in the ZBLAN:1%Er³++1%Ho³+ sample.

Keywords: Judd-Ofelt theory, up-conversion luminescence, visualization of IR radiation, fluoride glass, rare-earth elements.

DOI: 10.61011/EOS.2025.06.61665.6868-25

Introduction

Materials doped with rare-earth element (REE) ions are used in devices for generation, transmission, and control of optical signals. Lasers, fiber-optic amplifiers, phosphors, etc., are made based on them. Interest in such materials is also driven by the development of radiation visualizers for the near- and mid-infrared (IR) ranges (see, for example, [1–3]). This is related to the expanded use of IR lasers in experimental studies in molecular laser spectroscopy. The operating principle of such visualizers is based on the phenomenon of up-conversion luminescence of REE ions in amorphous or crystalline matrices [4,5].

Erbium and holmium are among the most widely used REEs. It is known that the presence of Er^{3+} ions in the matrix allows for the conversion of laser radiation with wavelengths in the 800, 975 and $1.55\,\mu\mathrm{m}$ regions into the visible range [6–8]. Additional doping with Ho^{3+} ions enables broadening the spectral visualization range. Recently, materials doped with Ho^{3+} ions have been used to visualize laser radiation in the two-micron range [9–11]. The wide absorption band of Ho^{3+} ions from the ground state on the $^5I_8 \rightarrow ^5I_7$ transition allows for luminescence excitation in the visible part of the spectrum under irradiation in the $1800-2150\,\mathrm{nm}$ range [12]. The need to visualize radiation in this range arose due to the use of near- and mid-IR lasers in environmental monitoring systems, clinical medicine, and other fields [13–15].

Donor-acceptor pairs of ions Yb³⁺-Er³⁺, Yb³⁺-Ho³⁺in particular, are used in up-conversion phosphors [1,16,17]. A large absorption cross-section at the ${}^2F_{7/2} \rightarrow {}^2F_{5/2}$ transition

of the Yb³⁺ donor ion compared to the acceptor and an increased in the ratio of the probability of excitation energy summation to the probability of cross-relaxation ensure a high output of up-conversion luminescence [5]. For example, the Yb³⁺-Er³⁺ pair efficiently converts IR radiation in the 1 μ m region into visible light at a wavelength of about 540 nm [18–20]. The Yb³⁺-Ho³⁺ pair exhibits up-conversion luminescence in the visible region at wavelengths of 540 and 650 nm under two-micron radiation [3,21,22].

Er³⁺ ions have a transition ${}^4I_{15/2} \rightarrow {}^4I_{11/2}$, whose energy is close to the energy of the Yb³⁺ ions ${}^2F_{7/2} \rightarrow {}^2F_{5/2}$ transition, making the study of up-conversion luminescence of the Er³⁺-Ho³⁺ ion pair at two-micron excitation interesting.

The efficiency of up-conversion strongly depends on the choice of matrix in which the ion is embedded. Usually, compounds with low probability of non-radiative multiphonon relaxation are used [23,24]. Such media include ZBLAN fluoride glass (ZrF₄-BaF₂-LaF₃-AlF₃-NaF) with high-frequency phonon energy of about $h\nu_{phon}\approx 575~\text{cm}^{-1}$ [18].

The aim of the present work was a theoretical and experimental study of the luminescent properties of ZBLAN: ${\rm Er^{3+}/Ho^{3+}}$ fluoride glass using the Judd-Ofelt model [25], as well as an analysis of up-conversion luminescence spectra of these samples under laser excitation at a wavelength of $1.94\,\mu{\rm m}$.

Theoretical part

To describe electronic transitions within the 4f-shell of RE ions, the theory proposed by Judd and Ofelt is

applied [26,27]. It allows calculating spontaneous emission probabilities, luminescence branching ratios, and radiative lifetimes.

The line strength of the electric dipole transition from an initial state $\langle \varphi_a |$ to all Stark components of the final state $|\varphi_b \rangle$ (assuming equal population of all Stark components of the initial state involved in transitions) is given by the formula:

$$S^{\text{calc}} = \sum_{i} \Omega_{i} \left| \langle \varphi_{a} \parallel U^{(i)} \parallel \varphi_{b} \rangle \right|^{2}, \tag{1}$$

where $\langle \varphi_a \parallel U^{(i)} \parallel \varphi_b \rangle$ are reduced matrix elements of unit tensor operators $U^{(i)}$ in the intermediate coupling approximation (values can be taken as independent of host matrix type; calculated for most RE ions [28,29]), Ω_i are Judd-Ofelt intensity parameters encoding dependence of transition intensities on the host matrix; odd parameters do not contribute. For electric dipole transitions, selection rules change accordingly. $\Delta S = 0$, $\Delta L \leq 6$, $\Delta J \leq 6$ ($\Delta J = 2$, 4, 6, if J or J' = 0). Thus, all information on RE ion emission intensity is contained in three parameters Ω_2 , Ω_4 , Ω_6 .

Judd-Ofelt parameters, as a set of phenomenological constants, are determined from experimental absorption cross-section data $\sigma(\lambda)$ from the ground state. The line strength of the electric dipole transition from the initial state $\langle J|$ to state $|I'\rangle$ can be expressed through the integral cross section on this transition:

$$S^{\exp} = \frac{3ch(2J+1)}{8\pi^3 e^{2\bar{\lambda}}} n \left(\frac{3}{n^2+2}\right)^2 \int \sigma(\lambda) d\lambda, \qquad (2)$$

where n is refractive index of the compound under examination, $\bar{\lambda}$ -is wavelength of the transition given by

$$\bar{\lambda} = \frac{\sum \lambda \sigma(\lambda)}{\sum \sigma(\lambda)}.$$
 (3)

This formula (2) is applicable when magnetic dipole transitions are forbidden by selection rules. Magnetic dipole selection rules are also defined. $\Delta S=0, \ \Delta L=0, \ \Delta J=0, \pm 1.$

The absorption cross-section dependence on wavelength is calculated from the transmission spectrum $T(\lambda)$. By definition, the transmittance of rare earth ions in the studied matrix is a dimensionless physical quantity equal to the ratio of the radiation intensity I, that reaches the output surface of the sample to the radiation intensity I_0 entering it. According to Bouguer's law, the output sample surface's intensity depends on sample thickness I as:

$$I = I_0 e^{-\alpha l},\tag{4}$$

where α —absorption coefficient, which can be expressed through the absorption cross-section and the concentration of REE ions in the matrix under study ($\alpha = \sigma n_{REE}$). Thus, we have the dependence of the absorption cross-section on the radiation wavelength:

$$\sigma(\lambda) = -\frac{\ln T(\lambda)}{n_{REF}l}.$$
 (5)

Formulas (1) and (2) allow determination of Judd-Ofelt parameters from experimental data by measuring REE ions transmission spectra in this matrix, calculating integral absorption cross-sections in the corresponding absorption bands, and calculating the strength of the transition lines using formula (2). Then, using the obtained values and formula (1), the least squares method can be used to find the parameters Ω_i . To assess the accuracy of the calculations, the total value of the root-mean-square deviation RMS for all line strengths is used, which is defined as follows:

$$RMS = \sqrt{\frac{\sum_{j=1}^{N} (S_{j}^{\text{exp}} - S_{j}^{\text{calc}})^{2}}{N - 3}},$$
 (6)

where N is the number of transitions observed in the absorption spectrum. Since there are only three Ω_i parameters, N must be greater than 3.

The Judd-Ofelt parameters allow us to find the probability of a spontaneous radiative transition A from the initial state $\langle J|$ to the state $|J'\rangle$:

$$A(J;J') = A_{ED} + A_{MD} = \frac{64\pi^4 e^2}{3h(2J+1)\bar{\lambda}^3} \times \left(n\left(\frac{n^2+2}{3}\right)^2 S_{ED} + n^3 S_M\right), \quad (7)$$

where A_{ED} and A_{MD} are the probabilities of spontaneous emission of electric and magnetic dipole transitions, E_{ED} and S_{MD} are the line strengths of the electric and magnetic dipole transitions. The line strength of the magnetic dipole transition is calculated by the formula:

$$S_{MD} = \left(\frac{h}{4\pi mc}\right)^{2} \left| \langle (S, L)J \parallel L + 2S \parallel (S', L')J' \rangle \right|^{2}, \quad (8)$$

where L + 2S — magnetic dipole operator of the transition $J \rightarrow J'$. The matrix element

$$\left| \left\langle (S,L)J \parallel L + 2S \parallel (S',L')J' \right\rangle \right|^2 \equiv M(J;J')$$

is calculated by the following formulas:

- for J' = J - 1:

$$M(J;J') = \frac{(S+L+J+1)(S+L+1-J)(J+S-L)(J+L-S)}{4J};$$
(9)

- for J' = J + 1:

$$M(J;J') = \frac{(S+L+J+2)(S+L-J)(J+1+S-L)(J+1+L-S)}{4(J+1)}.$$
(10)

If several radiative transitions are possible from the level under consideration, then the relative probability of a particular radiative transition can be determined from the total probability of radiative decay of this level, i.e. the luminescence branching coefficient β :

$$\beta = \frac{A(J;J')}{\sum_{J'} A(J;J')}.$$
(11)

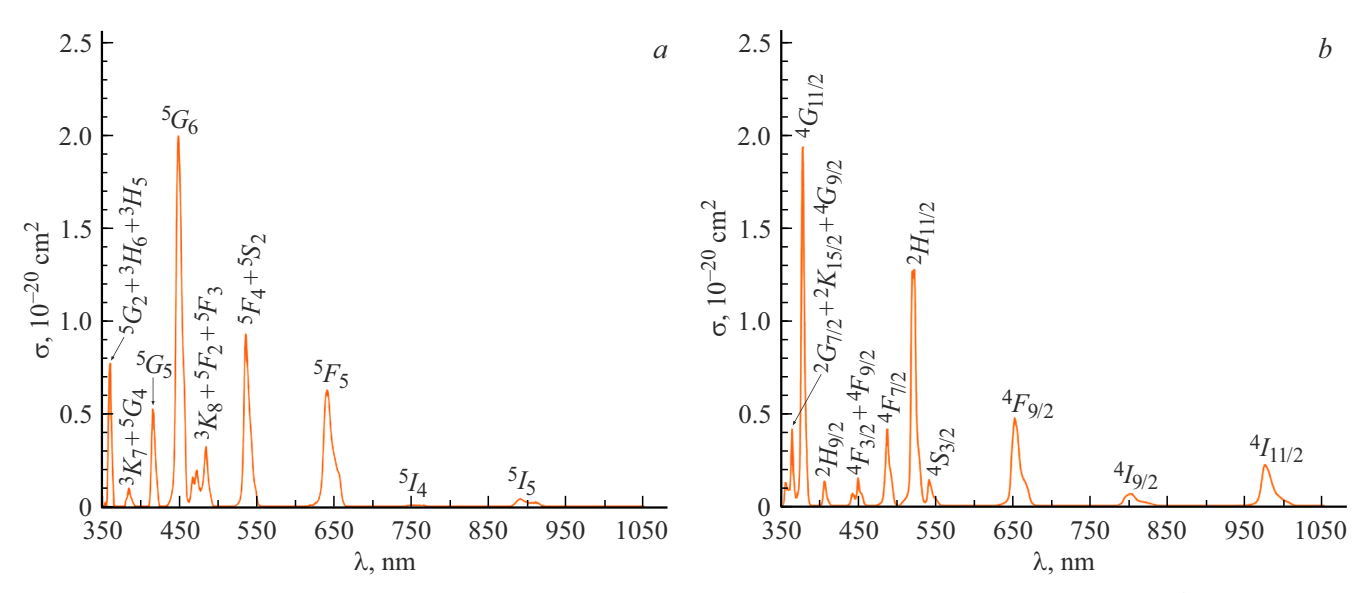


Figure 1. Spectral dependences of the absorption cross-section: from the ground state 5I_8 to excited multiplets of Ho³⁺ ions in ZBLAN glass (a), from the ground state ${}^4I_{15/2}$ to excited multiplets of Er³⁺ ions in ZBLAN glass (b).

Summation in formula (11) is performed over all radiative transitions from the initial state $\langle J|$. This sum determines the radiative lifetime of REE ions $\tau_{\rm rad}$ at the level of $\langle J|$:

$$\tau_{\text{rad}} = \frac{1}{\sum_{J'} A(J; J')}.$$
 (12)

Experimental part

ZBLAN glasses ($53ZrF_4$ - $20BaF_2$ - $4LaF_3$ - $3AlF_3$ -20NaF), doped with Er^{3+} , Ho^{3+} , Er^{3+}/Ho^{3+} ions were synthesized from the corresponding fluorides of "special purity" qualification in glassy carbon crucibles with a flowing inert atmosphere of nitrogen saturated with CCl₄ vapors, in a muffle furnace at a temperature of $800^{\circ}C$. The samples were molded in a dry glove box in a split aluminum mold. As a result, a series of fluoride glasses of the composition were prepared ZBLAN:1% Er^{3+} , ZBLAN:1% Er^{3+} + Er^{3+}

ZBLAN:1%Er³⁺+X%Ho³⁺ (X = 0.25, 0.5, 1 mol.%). For samples ZBLAN:1%Ho³⁺ ($n_{\text{Ho}} \approx 1.77 \cdot 10^{20} \text{ cm}^{-3}$, l = 2 mm) and ZBLAN:1%Er³⁺ ($n_{\text{Er}} \approx 1.77 \cdot 10^{20} \text{ cm}^{-3}$, l = 10 mm) the transmission spectra of the samples were measured using an SF-56 spectrophotometer, which were then recalculated using formula (5) as a function of the absorption cross section on the radiation wavelength.

To detect up-conversion luminescence, samples of the composition ZBLAN:1%Er³⁺+X%Ho³⁺ (X=0.25, 0.5, 1 mol.%) were used, which were alternately mounted on a holder. They were polished wafers of size $40 \times 10 \times 3 \text{ mm}^3$. A thulium laser (a Tm³⁺:YAP crystal with continuous diode pumping) generating radiation at a wavelength of $1.94 \, \mu \text{m}$ was used as an excitation source. During the measurement of the up-conversion luminescence spectra, the Tm³⁺:YAP-laser operated in the free-running mode. The average radiation power was about 2 W. Using

a short-focus lens, luminescence was collected at the entrance slit of a Solar M833 automated monochromator. A Thorlabs DET36A silicon photodiode (spectral sensitivity region 350–1100 nm rise time 14 ns) was placed behind the exit slit. A high signal-to-noise ratio was ensured by the method of synchronous signal detection. For this purpose, the luminescence emission was modulated by a Thorlabs MC1000A optical chopper with a frequency of 220 Hz, and the signal from the photodiode was detected at the same frequency using a Stanford Research Systems SR830 synchronous detector. Then the signal was fed to the ADC and then to the computer. The results were processed in the LabVIEW software environment.

Results and discussion

For $\mathrm{Ho^{3+}}$ and $\mathrm{Er^{3+}}$ ions in ZBLAN fluoride glass, the spectral dependences of the absorption cross section from the ground state (5I_8 for $\mathrm{Ho^{3+}}$ ions, ${}^4I_{15/2}$ for $\mathrm{Er^{3+}}$ ions) were obtained in the wavelength range of $350-1050\,\mathrm{nm}$ (Fig. 1, a and b respectively). In the figures, the level to which the transition occurs is indicated above each peak.

For the detected transitions of $\mathrm{Ho^{3+}}$ and $\mathrm{Er^{3+}}$ ions, the wavelengths and line strengths (refractive index of ZBLAN n=1.5 fluoride glass) were calculated using formulas (2) and (3). The results are given in Table 1. The squares of the matrix elements corresponding to these transitions [28] are also included in it. The calculated line strengths were related to electric dipole transitions, since magnetic dipole transitions between these levels are forbidden.

Based on the calculated transition parameters in accordance with the algorithm of the model under consideration, the Judd-Ofelt intensity parameters for the Ho³⁺ and Er³⁺ ions in the ZBLAN fluoride glass were found by the least

Ion	Transition		$\bar{\lambda}, \text{nm}$	S^{exp} , 10^{-20}cm^2	$ U^{(2)} ^2$	$ U^{(4)} ^2$	$ U^{(6)} ^2$
Ho ³⁺	$^5I_8 \rightarrow$	⁵ I ₅	897	0.120	0	0.0102	0.0930
		$^{5}I_{4}$	755	0.018	0	0.0000	0.0076
		$^{5}F_{5}$	643	1.950	0	0.4201	0.5701
		${}^{5}F_{4} + {}^{5}S_{2}$	538	2.177	0	0.2385	0.9235
		$^{3}K_{8} + ^{5}F_{2} + ^{5}F_{3}$	478	1.153	0.0205	0.0317	0.7040
		5G_6	449	5.522	1.4830	0.8201	0.1400
		5G_5	416	1.014	0	0.5239	0
		$^{3}K_{7}+^{5}G_{4}$	385	0.200	0.0056	0.0395	0.0667
		$^{3}H_{6}+^{3}H_{5}$	360	1.364	0.2540	0.2337	0.1609
		5G_2	353	0.012	0	0	0.0041
Er^{3+}	$^4I_{15/2} \rightarrow$	$^{4}I_{11/2}$	978	0.528	0.0276	0.0002	0.3942
		$^{4}I_{9/2}$	803	0.217	0	0.1587	0.0072
		$^{4}F_{9/2}$	653	1.265	0	0.5513	0.4621
		$^{4}S_{3/2}$	542	0.255	0	0	0.2225
		$^{2}H_{11/2}$	520	2.648	0.7158	0.4138	0.0927
		$^{4}F_{7/2}$	487	0.774	0	0.1465	0.6272
		$^{4}F_{3/2} + ^{4}F_{5/2}$	447	0.338	0	0	0.3476
		$^{2}H_{9/2}$	406	0.213	0	0.0243	0.2147
		$^{4}G_{11/2}$	377	3.391	0.9156	0.5263	0.1167
		$^{2}G_{7/2} + ^{2}K_{15/2} + ^{4}G_{9/2}$	362	0.794	0.0213	0.2576	0.3274

Table 1. Characteristics of transitions from the ground state in ZBLAN glasses doped with Ho³⁺ and Er³⁺ ions

Table 2. Judd-Ofelt intensity parameters for Ho³⁺ and Er³⁺ ions in ZBLAN glass

Ion	Ω_2 , 10^{-20} cm ²	Ω_4 , 10^{-20} cm ²	Ω_6 , 10^{-20} cm ²	RMS , 10^{-20} cm ²
Ho ³⁺	2.39	2.12	1.72	0.09
Er ³⁺	2.74	1.45	0.99	0.04

squares method (Table 2). A small value of the root-meansquare deviation of RMS relative to each of the parameters indicated the correctness of the estimates obtained.

The intensity parameters found for the ZBLAN:Ho3+ and ZBLAN:Er³⁺ compounds are in good agreement with the results of other authors. For example, for the ZBLAN:Ho³⁺, glass studied in [30], they had the following values

$$\begin{split} \Omega_2 &= (2.46 \pm 0.22) \cdot 10^{-20} \, \text{cm}^2, \\ \Omega_4 &= (2.02 \pm 0.39) \cdot 10^{-20} \, \text{cm}^2, \end{split}$$

$$\Omega_4 = (2.02 \pm 0.39) \cdot 10^{-20} \, \mathrm{cm}^2$$

$$\Omega_6 = (1.71 \pm 0.24) \cdot 10^{-20} \,\mathrm{cm}^2$$

and for ZBLAN:Er3+ glass studied in [31], —

$$\Omega_2 = (2.74 \pm 0.22) \cdot 10^{-20} \, \text{cm}^2$$

$$\Omega_4 = (1.47 \pm 0.40) \cdot 10^{-20} \, \text{cm}^2$$

$$\Omega_6 = (1.07 \pm 0.13) \cdot 10^{-20} \, \text{cm}^2$$
.

Using the obtained Judd-Ofelt parameters and formulas (1), (7)-(12)the spontaneous emission probabilities, luminescence branching coefficients and radiative lifetimes for excited states of Ho3+ and Er3+ ions in ZBLAN glass were calculated. The results obtained are given in Tables 3 and 4, respectively.

For the sample of the composed of ZBLAN:1%Er³⁺+1%Ho³⁺ the up-conversion luminescence spectrum was measured (Fig. 2). In the visible part of the spectrum, three bands were observed in the wavelength ranges of 515-560, 630-680 and 745-760 nm. The red

line at the wavelength of 655 nm had the highest intensity, corresponding to the ${}^4F_{9/2} \rightarrow {}^4I_{15/2}$ transitions of Er³⁺ and ${}^5F_5 \rightarrow {}^5I_8$ Ho³⁺ ions. The green band consisted of two peaks. The line with the wavelength of 520 nm belonged to the ${}^2H_{11/2} \rightarrow {}^4I_{15/2}$ transition of Er³⁺ions, and the line in the region of 545 nm corresponded to the ${}^4S_{3/2} \rightarrow {}^4I_{15/2}$ transitions of Er³⁺ ions and ${}^5S_2, {}^5F_4 \rightarrow {}^5I_8$ transitions of Ho³⁺ions. A weak band at the wavelength of 750 nm was due to the luminescence of Ho3+ ions into the first excited state at the 5S_2 , ${}^5F_4 \rightarrow {}^5I_7$ transition. In the ranges up to $1.1 \,\mu\text{m}$ two IR bands were also observed in the ranges of 880-930 and 945-1025 nm. The line in the region of 900 nm belonged to the ${}^5I_5 \rightarrow {}^5I_8$ transition of Ho³⁺ ions, and the line at a wavelength of 975 nm corresponded to the ${}^4I_{11/2} \rightarrow {}^4I_{15/2}$ transitions of Er³⁺ ions and ${}^5F_5 \rightarrow {}^5I_7$ transitions of Ho3+ions.

The ratios between the transition intensities corresponded to the luminescence branching coefficients calculated using the Judd-Ofelt theory (Tables 3 and 4), which confirmed the efficiency of its use for assessing the luminescent properties of materials doped with rare-earth ions.

concentration dependences of the conversion luminescence intensity were studied for ZBLAN:Er³⁺/Ho³⁺ fluoride glass. The spectra composed of ZBLAN:1%Ho³⁺, samples

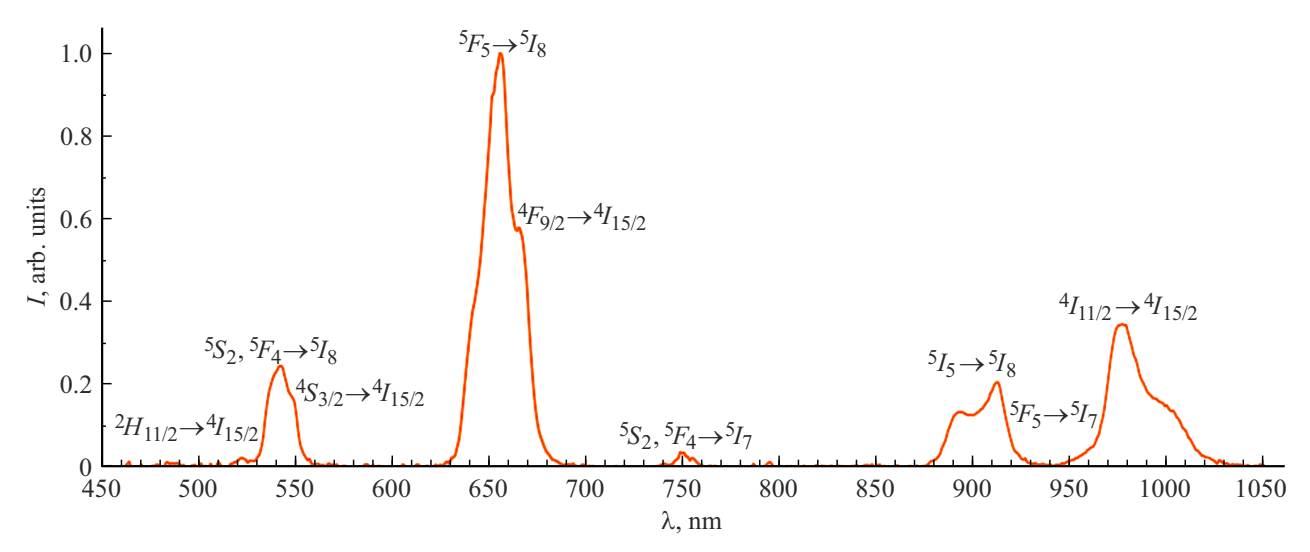


Figure 2. Up-conversion luminescence spectrum of the sample ZBLAN:1%Er³⁺+1%Ho³⁺.

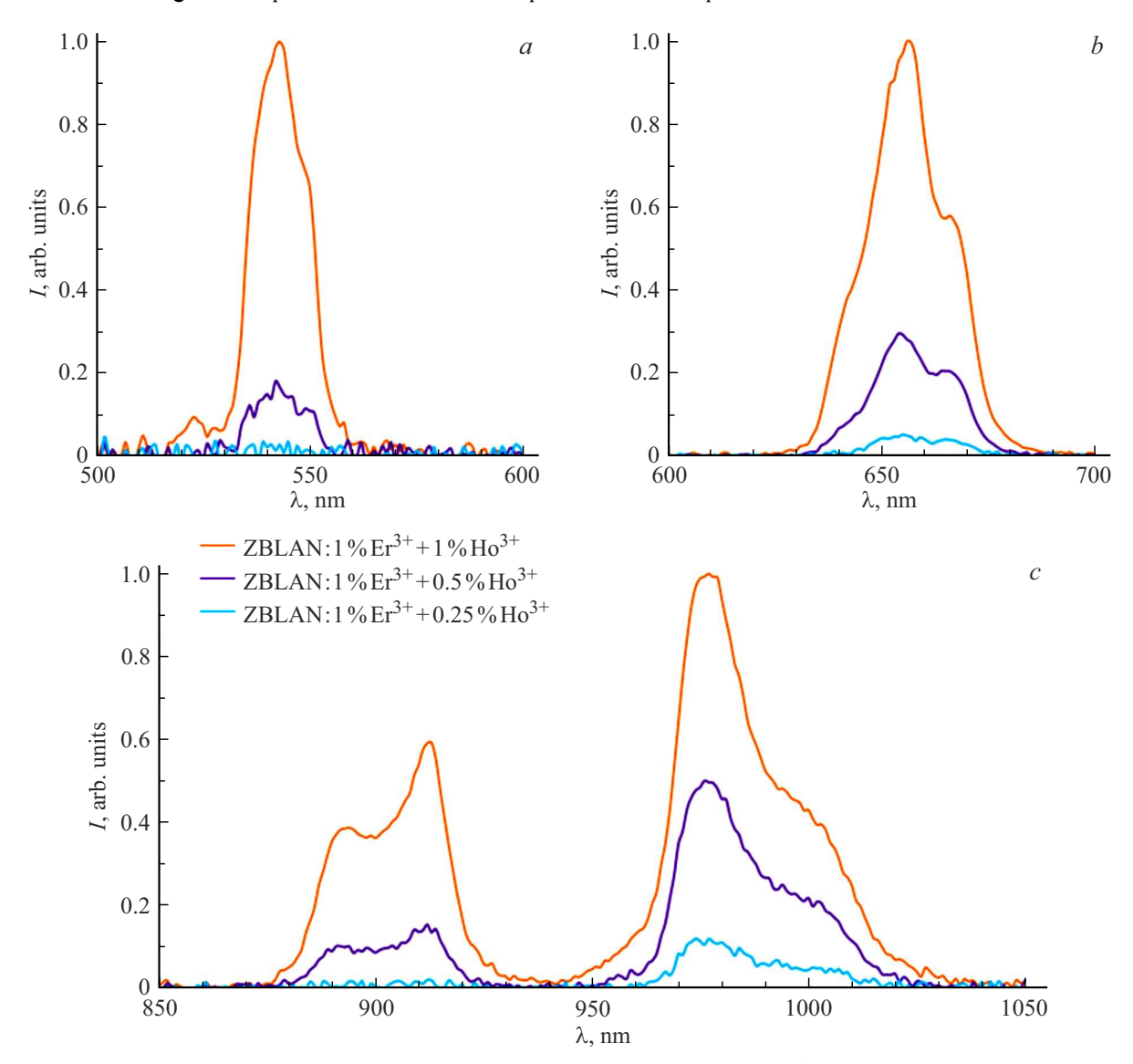


Figure 3. Up-conversion luminescence spectra of the samples ZBLAN:1% ${\rm Er^{3+}}+X$ % ${\rm Ho^{3+}}$ ($X=0.25,\,0.5,\,1\,{\rm mol.\%}$) in the ranges $500-600\,{\rm nm}$ (a), $600-700\,{\rm nm}$ (b) and $850-1050\,{\rm nm}$ (c).

Table 3. Spectroscopic characteristics of Ho³⁺ ions in ZBLAN glass

		I				
Transition		λ, nm	A_{ED} , s ⁻¹	$A_{MD}, {\rm s}^{-1}$	β	$ au_{rad}, \mu s$
Initial	Final					
state	state					
$^{5}I_{7}$	$^{5}I_{8}$	1946	58.24	21.00	1.000	12620
$^{5}I_{6}$	$^{5}I_{7}$	2809	14.72	11.91	0.158	5924
	$^{5}I_{8}$	149	142.19		0.842	
$^{5}I_{5}$	$^{5}I_{6}$	3945	4.66	5.05	0.074	7616
	$^{5}I_{7}$	1641	70.78		0.539	
	$^{5}I_{8}$	890	50.80		0.387	
$^{5}I_{4}$	$^{5}I_{5}$	4762	4.25	2.36	0.083	12530
	$^{5}I_{6}$	2157	28.98		0.363	
	$^{5}I_{7}$	1220	36.74		0.460	
	$^{5}I_{8}$	750	7.47		0.094	
⁵ <i>F</i> ₅	$^{5}I_{4}$	4415	0.04		0.000	550
	$^{5}I_{5}$	2291	5.86		0.003	
	$^{5}I_{6}$	1449	74.25		0.041	
	$^{5}I_{7}$	956	335.92		0.185	
	$^{5}I_{8}$	641	1402.04		0.771	
$^{5}S_{2}$	$^{5}F_{5}$	3509	0.35		0.000	519
	$^{5}I_{4}$	1955	32.28		0.017	
	$^{5}I_{5}$	1386	28.94		0.015	
	$^{5}I_{6}$	1026	121.36		0.063	
	$^{5}I_{7}$	751	738.35		0.383	
	$^{5}I_{8}$	542	1005.57		0.522	
$^{5}F_{4}$	$^{5}S_{2}$	41667	0.00		0.000	300
	$^{5}F_{5}$	3236	4.85	3.94	0.003	
	$^{5}I_{4}$	1867	18.32		0.005	
	$^{5}I_{5}$	1341	108.83		0.032	
	$^{5}I_{6}$	1001	202.40		0.061	
	$^{5}I_{7}$	738	283.15		0.085	
	$^{5}I_{8}$	535	2716.28		0.814	

ZBLAN:1%Er³⁺+X%Ho³⁺ (X = 0.25, 0.5, 1 mol.%) are shown in Figs. 3 and 4. The results of comparing the luminescence intensities of different samples are preliminary; measurements with an integrating sphere are required for a correct comparison.

With an increase in the concentration of $\mathrm{Ho^{3+}}$ ions, the luminescence intensity increased (Fig. 3). In this case, the qualitatively observed picture did not change — the shape of the spectrum was preserved. This was due to the fact that it was the $\mathrm{Ho^{3+}}$ ions that provided the first excitation step, since only they have an absorption band from the ground state in the wavelength region of $1.94\,\mu\mathrm{m}$ (the $\mathrm{Er^{3+}}$ ions do not have such a band).

Addition of Er^{3+} ions led to a significant change in the luminescence spectrum. The intensity of the red band increased significantly (Fig. 4, b). At the same time, the width of the spectrum increased due to the appearance of transitions of Er^{3+} ions. A similar picture was observed for the green band (Fig. 4, a), as well as for the IR band in the

Table 4. Spectroscopic characteristics of Er³⁺ ions in ZBLAN glass

Trans	sition	λ, nm	A_{ED} , s ⁻¹	A_{MD} , s ⁻¹	β	$ au_{rad}, \mu s$
Initial			,	, ,	,	,
state	state					
$^{4}I_{13/2}$	$^{4}I_{15/2}$	1530	71.26	34.82	1.000	9427
$^{4}I_{11/2}$	$^{4}I_{13/2}$	2674	13.47	10.07	0.204	8671
	$^{4}I_{15/2}$	973	91.79		0.796	
$^{4}I_{9/2}$	$^{4}I_{11/2}$	4525	0.60	1.87	0.018	7371
	$^{4}I_{13/2}$	1681	32.87		0.242	
	$^{4}I_{15/2}$	801	100.32		0.739	
$^{4}F_{9/2}$	$^{4}I_{9/2}$	3448	1.93		0.002	917
	$^{4}I_{11/2}$	1957	42.58		0.039	
	$^{4}I_{13/2}$	1130	50.36		0.046	
	$^{4}I_{15/2}$	650	995.36		0.913	
$^{4}S_{3/2}$	$^{4}F_{9/2}$	3190	0.38		0.000	871
-,	$^{4}I_{9/2}$	1657	43.69		0.038	
	$^{4}I_{11/2}$	1213	25.34		0.022	
	${}^{4}I_{13/2}$	834	317.32		0.276	
	$^{4}I_{15/2}$	540	761.96		0.663	
$^{2}H_{11/2}$	${}^{4}S_{3/2}$	14815	0.02		0.000	279
,-	${}^{4}F_{9/2}$	2625	10.77		0.003	
	$^{4}I_{9/2}$	1490	49.87		0.014	
	$^{4}I_{11/2}$	1121	42.97		0.012	
	$^{4}I_{13/2}$	790	75.09		0.021	
	$^{4}I_{15/2}$	521	3402.87		0.950	
$^{4}F_{7/2}$	$^{2}H_{11/2}$	7246	0.55		0.000	382
,,2	${}^{4}S_{3/2}$	4866	0.02		0.000	
	${}^{4}F_{9/2}$	1927	3.70	15.90	0.007	
	${}^{4}I_{9/2}$	1236	87.51		0.033	
	${}^{4}I_{11/2}$	971	162.28		0.062	
	${}^{4}I_{13/2}$	712	369.87		0.141	
	$^{4}I_{15/2}$	486	1975.06		0.755	
	113/2	100	1775.00		5.755	

region of 975 nm (Fig. 4, c). The IR luminescence spectrum in the region of 900 nm remained virtually unchanged.

To assess the efficiency of conversion of two-micron radiation into the visible range by ZBLAN:Er³+/Ho³+ glass, Fig. 5 shows the up-conversion luminescence spectrum of the most intense sample of this series ZBLAN:1%Er³++1%Ho³+ in comparison with the spectrum of the ZBLAN:1%Ho³++3%Yb³+ compound, which has already established itself as a good visualizer of radiation in the 2 μ m region [32]. The intensity of the red band in the ZBLAN:1%Er³++1%Ho³+ sample was somewhat lower, but the band itself was wider. Thus, the yield of red luminescence in the glasses under consideration was practically the same. This allows us to recommend the ZBLAN:1%Er³++1%Ho³+ compound for use as a radiation visualizer in the 2 μ m region.

The threshold power density of the Tm^{3+} :YAP-laser ($\lambda = 1.94 \, \mu m$) radiation visualization decreased with increasing Ho^{3+} ion concentration and in the ZBLAN:1%Er³⁺+1%Ho³⁺ glass was 30 W/cm². This value can be significantly reduced if optical ceramics are obtained

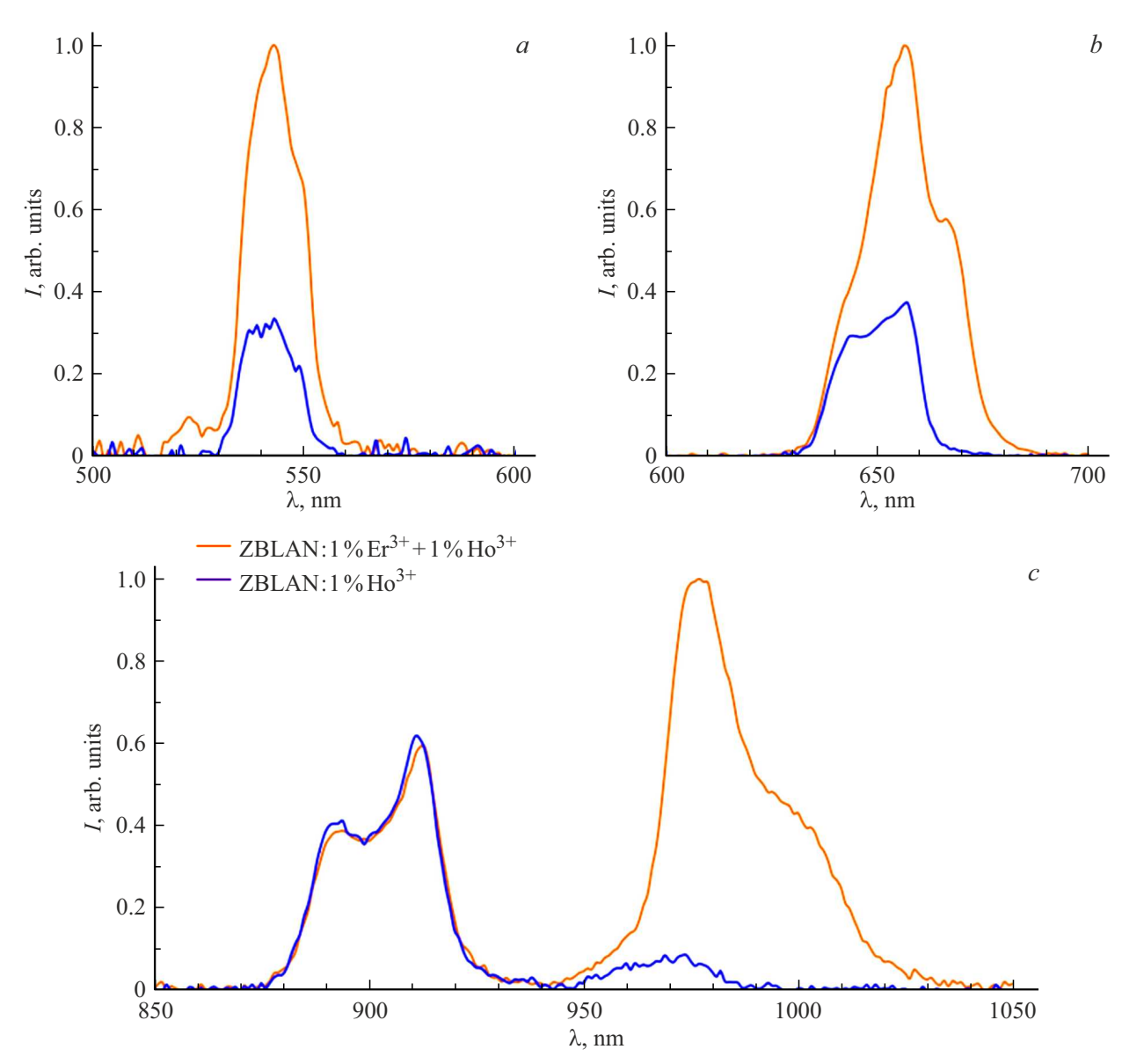


Figure 4. Up-conversion luminescence spectra of the ZBLAN: $1\%\text{Er}^{3+}+1\%\text{Ho}^{3+}$ and ZBLAN: $1\%\text{Ho}^{3+}$ samples in the ranges $500-600\,\text{nm}$ (a), $600-700\,\text{nm}$ (b) and $850-1050\,\text{nm}$ (c).

from the glass by thermal treatment. For example, in [32] a decrease in the threshold power density of visualization of Tm³+:YLF-laser radiation ($\lambda=1.908\,\mu\text{m}$) in ceramic samples of the ZBLAN:1%Ho³++3%Yb³+ composition by 150 times was found compared to the original glass samples. This is due to the fact that thermal annealing of glasses often leads to a significant enhancement of luminescence (by tens of times) due to the release of a crystalline phase (see, for example [33,34]); in ZBLAN fluoride glasses, a crystalline phase β -BaZrF₆ is formed [35].

Conclusion

A study was conducted on the luminescent properties of ZBLAN fluoride glass doped with Er³⁺ and Ho³⁺ions.

For the compounds ZBLAN:1%Ho³+ and ZBLAN:1%Er³+ transmission spectra were measured, based on which, according to the Judd-Ofelt model algorithm for Ho³+and Er³+ ions in ZBLAN fluoride glass, intensity parameters were found and spontaneous emission probabilities, branching ratios of luminescence, and radiative lifetimes were calculated. Up-conversion luminescence spectra were measured for samples with compositions ZBLAN:1%Ho³+, ZBLAN:1%Er³++X%Ho³+ (X=0.25,0.5,1 mol.%) under excitation by Tm³+:YAP-laser radiation at a wavelength of 1.94 μ m. The addition of Er³+ ions contributed to a significant increase in up-conversion efficiency. The most intense luminescence band was the red band at a wavelength of 655 nm, corresponding to the transitions ${}^4F_{9/2} \rightarrow {}^4I_{15/2}$ of Er³+ ions and ${}^5F_5 \rightarrow {}^5I_8$ of Ho³+ ions. With an

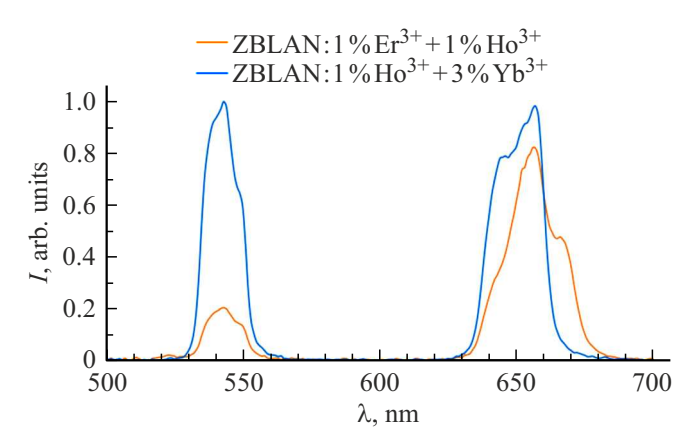


Figure 5. Up-conversion luminescence spectra of the samples $ZBLAN:1\%Er^{3+}+1\%Ho^{3+}$ and $ZBLAN:1\%Ho^{3+}+3\%Yb^{3+}$.

increase in $\mathrm{Ho^{3+}}$ ion concentration, the luminescence intensity increased, the red emission visualization threshold decreased, and in the glass ZBLAN:1%Er³++1%Ho³+ it amounted to 30 W/cm².

Funding

This study was supported by the national project "Science and Universities" (project FSWR-2024-0004) funded by the federal budget subsidy for the financial support of the state assignment for scientific research.

Conflict of interest

The authors declare that they have no conflict of interest.

References

- [1] F. Auzel, D. Pecile, D. Morin. J. Electrochem. Soc., **122** (1), 101 (1975). DOI: 10.1149/1.2134132
- A.P. Savikin, A.V. Budruev, A.N. Shushunov, E.L. Tikhonova,
 K.V. Shastin, I.A. Grishin. Inorg. Mater., 50 (11), 1169 (2014).
 DOI: 10.1134/S0020168514110156.
- [3] A.P. Savikin, A.S. Egorov, A.V. Budruev,
 I.A. Grishin. Opt. Spectrosc., 120 (6), 902 (2016).
 DOI: 10.1134/S0030400X16060199.
- [4] F. Auzel. Proc. IEEE, 61 (6), 758 (1973).DOI: 10.1109/PROC.1973.9155
- [5] A.K. Kazaryan, Yu.P. Timofeev, M.V. Fok. V sb.: Centry svecheniya redkozemel'nyh ionov v kristallofosforah, edited by N.G. Basov. (in Russian) Trudy FIAN (Nauka, M., 1986), v. 175. p. 4.
- [6] M. Tsuda, K. Soga, H. Inoue, S. Inoue, A. Makishima. J. Appl. Phys., 85 (1), 29 (1999). DOI: 10.1063/1.369445
- [7] T. Danger, J. Koetke, R. Brede, E. Heumann, G. Huber,
 B.H.T. Chai. J. Appl. Phys., 76 (3), 1413 (1994).
 DOI: 10.1063/1.357745
- [8] J. Zhao, L. Wu, C. Zhang, B. Zeng, Y. Lv, Z. Li, Q. Jiang,
 Z. Guo. J. Mater. Chem. C, 5 (16), 3903 (2017).
 DOI: 10.1039/C7TC00757D

- [9] A.A. Lyapin, P.A. Ryabochkina, S.N. Ushakov, P.P. Fedorov. Quantum Electron., 44 (6), 602 (2014).DOI: 10.1070/QE2014v044n06ABEH015423.
- [10] A.P. Savikin, A.S. Egorov, A.V. Budruev, I.Yu. Perunin,
 I.A. Grishin. Tech. Phys. Lett., 42 (11), 1083 (2016).
 DOI: 10.1134/S1063785016110079.
- [11] P.P. Fedorov, A.A. Luginina, S.V. Kuznetsov, V.V. Voronov, A.A. Lyapin, A.S. Ermakov, D.V. Pominova, A.D. Yapryntsev, V.K. Ivanov, A.A. Pynenkov, K.N. Nishchev. Cellulose, 26 (4), 2403 (2019). DOI: 10.1007/s10570-018-2194-4
- [12] A.A. Lyapin, P.A. Ryabochkina, S.N. Ushakov, V.V. Osiko, P.P. Fedorov, A.A. Demidenko, E.A. Garibin. it Sposob vizualizacii dvuhmikronnogo lazernogo izlucheniya v vidimyj svet. Patent RU 2549561 C1, 27.04.2015. (in Russian)
- [13] I. Kaplan, D. Aravot, S. Giler, Y. Gat, D. Sagie, Y. Kagan. In: LASER Optoelectronics in Medicine, ed. by W. Waidelich, R. Waidelich. (Springer, Heidelberg, 1988), p. 23. DOI: 10.1007/978-3-642-72870-9_6
- [14] S. Wenk, S. Fürst, V. Danicke, D.T. Kunde. In: Advances in Medical Engineering, ed. by T.M. Buzug, D. Holz, J. Bongartz, M. Kohl-Bareis, U. Hartmann, S. Weber. Springer Proceedings in Physics (Springer, Heidelberg, 2007), vol. 114, p. 447. DOI: 10.1007/978-3-540-68764-1_75
- [15] B.M. Walsh. Laser Phys., 19 (4), 855 (2009). DOI: 10.1134/S1054660X09040446
- [16] K. Lemański, R. Pazik, P.J. Dereń. Opt. Mater., 34 (12), 1990 (2012). DOI: 10.1016/j.optmat.2011.12.021
- [17] W. Xu, X. Gao, L. Zheng, Z. Zhang, W. Cao. Opt. Express, 20 (16), 18127 (2012). DOI: 10.1364/OE.20.018127
- [18] I.A. Grishin, V.A. Guryev, A.P. Savikin, N.B. Zvonkov. Opt. Fiber. Tech., *I* (4), 331 (1995). DOI: 10.1006/ofte.1995.1027
- [19] K. Anders, A. Jusza, P. Komorowski, P. Andrejuk, R. Pirami-dowicz. J. Lumin., 201, 427 (2018).
 DOI: 10.1016/j.jlumin.2018.04.056
- [20] D.Y. Wang, P.C. Ma, J.C. Zhang, Y.H. Wang. ACS Appl. Energy Mater., 1 (2), 447 (2018). DOI: 10.1021/acsaem.7b00093
- [21] A.P. Savikin, K.E. Sumachev, I.A. Grishin, V.V. Sharkov.
 J. Non-Cryst. Solids, 572, 121087 (2021).
 DOI: 10.1016/j.jnoncrysol.2021.121087
- [22] A.P. Savikin, I.Yu. Perunin, S.V. Kurashkin, A.V. Budruev, I.A. Grishin. Opt. Spectrosc., 124 (3), 307 (2018). DOI: 10.1134/S0030400X18030190.
- [23] T. Miyakawa, D.L. Dexter. Phys. Rev. B, 1 (7), 2961 (1970). DOI: 10.1103/PhysRevB.1.2961
- [24] F. Auzel. Phys. Rev. B, 13 (7), 2809 (1976).DOI: 10.1103/PhysRevB.13.2809
- [25] B.M. Walsh. In: Advances in Spectroscopy for Lasers and Sensing, ed. by B. Bartolo, O. Forte. NATO Science Series II: Mathematics, Physics and Chemistry (Springer, Dordrecht, 2006), vol. 231, p. 403. DOI: 10.1007/1-4020-4789-4_21
- [26] B.R. Judd. Phys. Rev., 127 (3), 750 (1962).DOI: 10.1103/PhysRev.127.750
- [27] G.S. Ofelt. J. Chem. Phys., **37** (3), 511 (1962). DOI: 10.1063/1.1701366
- [28] W.T. Carnall, H. Crosswhite, H.M. Crosswhite. *Energy Level Structure and Transition Probabilities in the Spectra of the Trivalent Lanthanides in LaF*₃ (Argonne National Laboratory, Lemont, 1978). DOI: 10.2172/6417825
- [29] W.T. Carnall, P.R. Fields, K. Rajnak. J. Chem. Phys., 49 (10), 4424 (1968). DOI: 10.1063/1.1669893

- [30] D. Piatkowski, K. Wisniewski, M. Rozanski, Cz. Koepke, M. Kaczkan, M. Klimczak, R. Piramidowicz, M. Malinowski. J. Phys.: Condens. Matter, 20 (15), 155201 (2008). DOI: 10.1088/0953-8984/20/15/155201
- [31] D. Piatkowski, K. Wisniewski, M. Rozanski, Cz. Koepke. Phys. Procedia, 2 (2), 365 (2009). DOI: 10.1016/j.phpro.2009.07.021
- [32] A.P. Savikin, A.S. Egorov, A.V. Budruev, I.A. Grishin. Glass Physics and Chemistry, 42 (5), 473 (2016). DOI: 10.1134/S108765961605014X.
- [33] R. Lisiecki, E. Czerska, M. Żelechower, R. Swadźba, W. Ryba-Romanowski. Mater. Des., 126, 174 (2017). DOI: 10.1016/j.matdes.2017.04.046
- [34] G. Arzumanyan, V. Vartic, A. Kuklin, D. Soloviov, G. Rachkovskaya, G. Zacharevich, E. Trusova, N. Skoptsov, K. Yumashev. J. Phys. Sci. Appl., 4 (3), 150 (2014).
- [35] L. Qin, Z.X. Shen, B.L. Low, H.K. Lee, T.J. Lu, Y.S. Dai, S.H. Tang, M.H. Kuok. J. Raman Spectrosc., 28 (7), 495 (1997). DOI: 10.1002/(SICI)1097-4555(199707)28:7;495::AID-JRS116;3.0.CO;2-X

Translated by J.Savelyeva